

Directed Evolution of Soluble Single-chain Human Class II MHC Molecules

Olga Esteban¹ and Huimin Zhao^{1,2,3,4*}

¹Department of Chemical and Biomolecular Engineering
University of Illinois at Urbana-Champaign
600 S. Mathews Ave
Urbana, IL 61801, USA

²Department of Chemistry
University of Illinois at Urbana-Champaign
600 S. Mathews Ave
Urbana, IL 61801, USA

³Center for Biophysics and Computational Biology
University of Illinois at Urbana-Champaign
600 S. Mathews Ave
Urbana, IL 61801, USA

⁴Department of Bioengineering
University of Illinois at Urbana-Champaign
600 S. Mathews Ave
Urbana, IL 61801, USA

Major histocompatibility complex (MHC) class II molecules are membrane-anchored heterodimers that present antigenic peptides to T cells. Expression of these molecules in soluble form has met limited success, presumably due to their large size, heterodimeric structure and the presence of multiple disulfide bonds. Here we have used directed evolution and yeast surface display to engineer soluble single-chain human lymphocyte antigen (HLA) class II MHC DR1 molecules without covalently attached peptides (scDR1 $\alpha\beta$). Specifically, a library of mutant scDR1 $\alpha\beta$ molecules was generated by random mutagenesis and screened by fluorescence activated cell sorting (FACS) with DR-specific conformation-sensitive antibodies, yielding three well-expressed and properly folded scDR1 $\alpha\beta$ variants displayed on the yeast cell surface. Detailed analysis of these evolved variants and a few site-directed mutants generated *de novo* indicated three amino acid residues in the β 1 domain are important for the improved protein folding yield. Further, molecular modeling studies suggested these mutations might increase the protein folding efficiency by improving the packing of a hydrophobic core in the α 1 β 1 domain of DR1. The scDR1 $\alpha\beta$ mutants displayed on the yeast cell surface are remarkably stable and bind specifically to DR-specific peptide HA_{306–318} with high sensitivity and rapid kinetics in flow cytometric assays. Moreover, since the expression, stability and peptide-binding properties of these mutants can be directly assayed on the yeast cell surface using immuno-fluorescence labeling and flow cytometry, time-consuming purification and refolding steps of recombinant DR1 molecules are eliminated. Therefore, these scDR1 $\alpha\beta$ molecules will provide a powerful technology platform for further design of DR1 molecules with improved peptide-binding specificity and affinity for therapeutic and diagnostic applications. The methods described here should be generally applicable to other class II MHC molecules and also class I MHC molecules for their functional expression, characterization and engineering.

© 2004 Elsevier Ltd. All rights reserved.

*Corresponding author

Keywords: directed evolution; yeast display; fluorescence activated cell sorting (FACS); major histocompatibility complex (MHC); protein folding

Introduction

Human major histocompatibility complex (MHC) class II molecules bind peptide antigens and present them to T cell receptors (TCRs) of CD4⁺ T cells in cell-mediated immunity.¹ These

MHC proteins have been linked to a variety of human diseases, including multiple sclerosis, rheumatoid arthritis, type I diabetes, transplant rejection and certain infectious diseases such as malaria.^{2,3} A detailed understanding of their biological role in immune responsiveness has spurred the design of MHC-based reagents that might be used as immunospecific human therapeutics and diagnostics. For example, soluble MHC class I tetramers were used to modulate an antigen-specific T cell response *in vivo*,⁴ whereas soluble peptide–MHC class II complexes were shown to

Abbreviations used: MHC, major histocompatibility complex; FACS, fluorescence activated cell sorting; HLA, human lymphocyte antigen; TCRs, T cell receptors.

E-mail address of the corresponding author:
zhao5@uiuc.edu

control the activity of autoreactive T cells associated with Type I diabetes^{5,6} and experimental allergic encephalomyelitis.⁷ In addition, detection of a variety of antigen-specific human T cells has been accomplished using multivalent soluble peptide–MHC complexes.⁸

A positive correlation between the affinity of peptide tightly bound to MHC molecules and *in vivo* immunogenicity for generating potent T-cell responses has been described in a number of experimental murine and human studies.^{9,10} It was also found that stronger affinities of particular peptides for their MHC-presenting elements result in more stable tetramer reagents.¹¹ Thus, MHC molecules with increased peptide-binding affinity and specificity are highly desired for successful development of MHC-based therapeutic and diagnostic agents. Unfortunately, a major drawback in the design of MHC-based reagents with improved affinity and specificity is the lack of a convenient and efficient system that expresses soluble and functional MHC molecules and is amenable to powerful protein engineering approaches such as directed evolution. As an alternative approach to structure-based rational design, directed evolution involves random mutagenesis and gene recombination followed by high throughput screening or selection and is very effective in engineering proteins with novel or improved functions, such as affinity, activity, stability, and selectivity.^{12,13} In particular, directed evolution has been demonstrated to be very effective in overcoming the bottlenecks of functional expression of proteins in soluble form.^{14–16} Expression of soluble MHC class II molecules has met limited success mainly due to their large size, heterodimeric structure, and the presence of multiple disulfide bonds. Some of these molecules have been difficult to express due to the failure of MHC class II α and β -chains to assemble and/or due to a strong tendency for molecules to aggregate. For example, leucine zippers were required to force the pairing of α and β -chain of DR2¹⁷ and I-A¹⁸ in the absence of their transmembrane regions. Conversely, extracellular domains of α and β -chains from other class II molecules such as DR1 and DR4 have been expressed and assembled as soluble heterodimeric proteins in insect cells,^{19–21} but such expression system is not amenable to directed evolution.

To overcome this drawback, we have used yeast cell surface display and directed evolution. Yeast surface display allows expression of a protein of interest as a fusion protein with the yeast AGA2 agglutinin mating factor on the cell surface.²² It is an efficient system for directed evolution since a library of protein variants can be readily generated and screened by fluorescence-activated cell sorting (FACS)²³ or magnetic beads,²⁴ and it offers multiple advantages over other display methods such as phage display.²⁵ Yeast is a eukaryote and therefore contains protein-processing machinery similar to that of a mammalian cell. Thus, yeast is more appropriate than prokaryotes to correctly express

and display human therapeutic proteins, including MHC molecules. Moreover, the robustness of the yeast surface provides an excellent scaffold for direct biochemical and biophysical characterization of the displayed protein. Yeast surface display coupled with sorting by flow cytometry or magnetic beads has been used to engineer single-chain antibodies,^{26–28} single-chain TCR receptors of increased affinity and stability,^{29–32} stabilized versions of class II I-A³³, and more recently, tumor necrosis factor- α (TNF- α) mutants with higher expression levels.³⁴ However, expression of “functionally empty” class II molecules capable of binding exogenously added antigenic peptides has yet to be demonstrated.

Here we used directed evolution coupled with yeast cell surface display to engineer single-chain human class II MHC DR1 protein variants without covalently linked peptides that are remarkably stable, well-expressed and capable of binding DR-specific peptides on the yeast cell surface with high sensitivity and rapid kinetics in flow cytometric assays. These scDR1 $\alpha\beta$ variants contain specific mutations located in the β 1 domain which increase the folding yield of the DR1 molecules by presumably improving the packing of a hydrophobic core in the α 1 β 1 domain. The yeast display system developed in this work could substitute for conventional cellular-binding assays with antigen presenting cells to investigate structural requirements for binding of peptides to cell surface class II MHC molecules. More importantly, this system provides a basis for further engineering of MHC-based diagnostic and therapeutic agents for the treatment of autoimmune diseases, cancers and infectious diseases.

Results

Expression and detection of wild-type scDR1 molecule on the yeast cell surface

To evaluate the expression of wild-type HLA-DR1 molecule in the yeast display system, genes encoding the single-chain DR1 constructs, scDR1 $\alpha\beta$ (α -linker- β) or scDR1 $\beta\alpha$ (β -linker- α), were cloned into the yeast pYD1 display vector as an AGA2 polypeptide fusion (Figure 1). Analysis of expression of Xpress and V5 epitope tags that flank the single-chain DR1 constructs by flow cytometry allowed the estimation of yeast surface expression levels. A positive staining population was detected with the anti-Xpress (data not shown) and anti-V5 antibodies (Figure 2). A similar number of positive cells were observed for both tags, indicating that all positive cells had expressed the full-length protein, and unlike other heterologous eukaryotic proteins expressed in a similar system,^{32,33} no significant proteolytic cleavage to the carboxyl end of the fused protein had occurred. The surface expression level of scDR1 $\alpha\beta$ or scDR1 $\beta\alpha$ was very high, as indicated by the

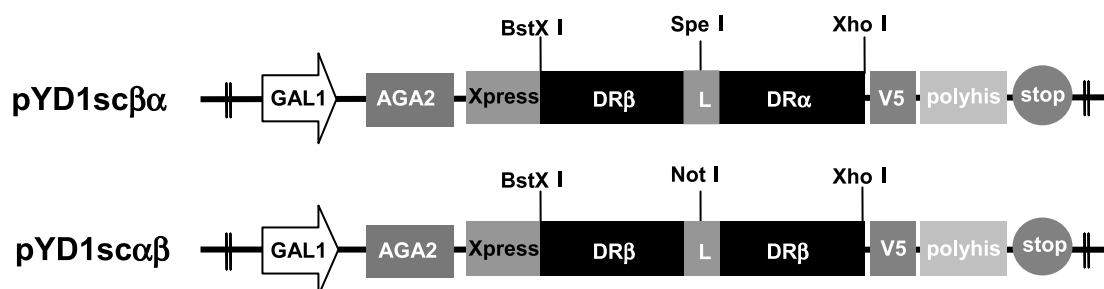


Figure 1. Schematic representation of the single-chain HLA-DR1 constructs used for yeast cell surface display. V5 = V5 epitope, Xpress = Xpress epitope, L = linker region.

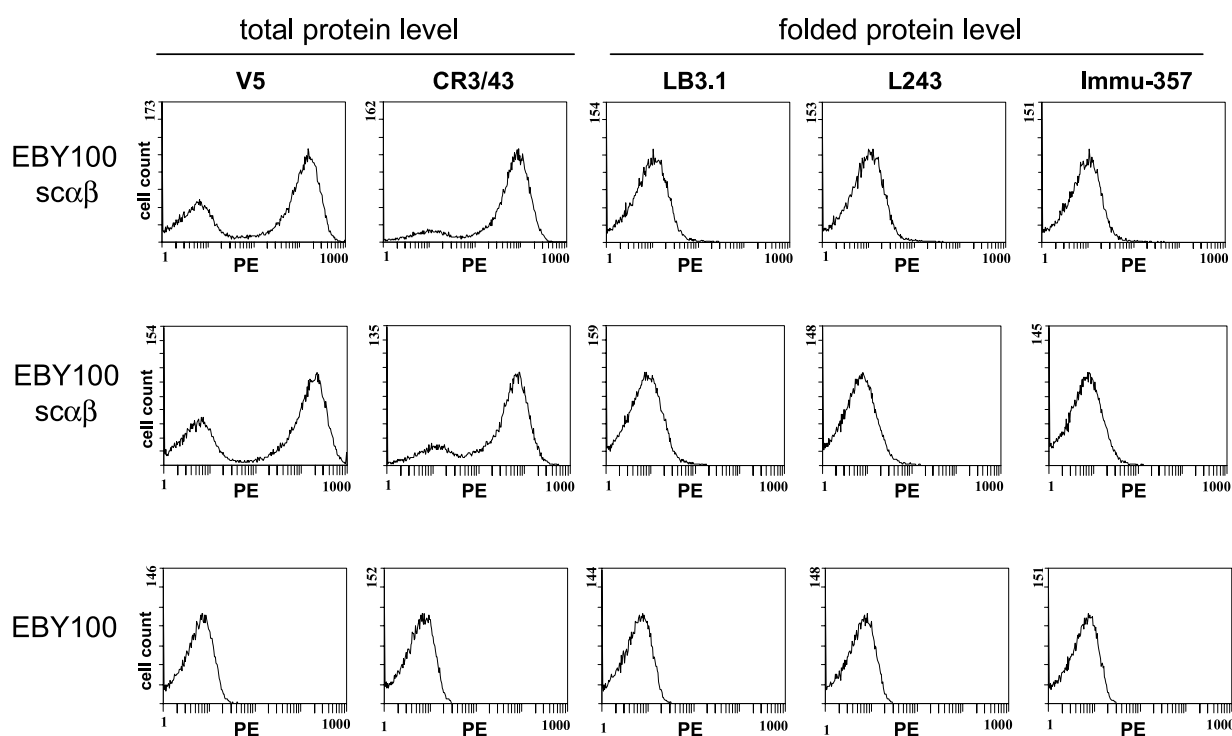


Figure 2. Histograms showing fluorescence of cells displaying the wild-type scDR1 $\alpha\beta$ and scDR1 $\beta\alpha$ molecules. Cells were labeled with anti-V5, anti-DR CR3/43, LB3.1, L243, Immu-357 antibodies followed by secondary labeling with biotinylated goat-anti-mouse IgG and SA-PE, and then analyzed by flow cytometry. The two first columns correspond to histograms of cells stained with antibodies anti-V5 and CR3/43, which recognize a linear epitope in the wild-type scDR1 proteins. The three right columns represent histograms of cells stained with the conformation-sensitive DR-specific antibodies LB3.1, L243 and Immu-357. As judged by the low reactivity against these antibodies of the yeast cells displaying wild-type scDR1 molecules, no folded protein is seen with wild-type scDR1 molecules. Approximately 75% of the population of cells expressed scDR1 $\alpha\beta$ on the surface. Labeled yeast cells were analyzed on a Coulter Epics XL flow cytometer collecting 30,000 cells gated on light scatter (size) to prevent analysis of the clumps.

fluorescence intensity obtained with the V5 antibody (mean fluorescence units (MFU) = 121.0). Expression of properly folded wild-type scDR1 $\alpha\beta$ or scDR1 $\beta\alpha$ on the yeast cell surface, however, could barely be detected by conformation-sensitive anti-DR antibodies including L243, LB3.1, and Immu-357 (MFU = 1.5–1.8, compared to 0.6 for yeast cells without expressing scDR1 $\alpha\beta$) (Figure 2). It is noteworthy that the L243 and LB3.1 antibodies can only recognize correctly assembled DR heterodimers.^{21,35} On the other hand, binding of the wild-type single-chain DR1 molecules to the

DR-specific antibody, CR3/43, which recognizes denatured β -chain of DR molecules, could be detected by flow cytometry (Figure 2). It should be noted that the negative population observed in histograms corresponds to yeast cells in a specific stage of the cell cycle that do not express high levels of the fusion protein. This negative population has been observed for all yeast displayed proteins.^{22,36}

Binding of the surface-displayed AGA2-scDR1 fusion proteins to CR3/43 was also confirmed by immunoblot analysis (Figure 3). A band specific

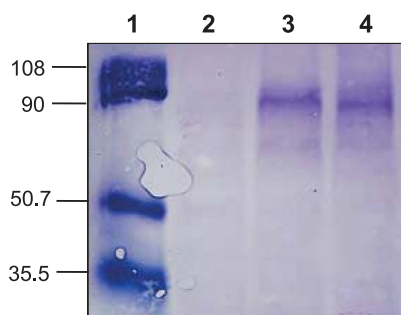


Figure 3. Immunoblot analysis of single-chain HLA-DR1 fusion proteins probed with the anti-DR, -DP and -DQ β -chain mAb CR3/43. The molecular masses of the protein markers are shown on the left. Lane 1: prestained low-range marker, lane 2: AGA2-V5 protein (negative control), lane 3: AGA2-sc $\beta\alpha$, and lane 4: AGA2-sca β . Although the predicted molecular mass of AGA2 is under 7 kDa, AGA2 has an apparent molecular mass of 33 kDa because of its extensive glycosylation.³⁷

to the yeast cells displaying the wild-type single-chain DR1 molecules was observed, which corresponds to a protein with an apparent molecular mass of ≈ 90 kDa. This apparent molecular mass is ≈ 30 kDa larger than the expected size of the AGA2-DR1 fusion protein, indicating the fusion protein is glycosylated. Indeed, although the predicted molecular mass of AGA2 is under 7 kDa, AGA2 was found to have an apparent molecular mass of 33 kDa on SDS-polyacrylamide gels because of its extensive O-glycosylation.³⁷ Together, these data indicated that the wild-type scDR1 could be expressed on the yeast cell surface at high levels but not in their native state.

Directed evolution of folded scDR1 $\alpha\beta$ variants with increased expression level

To obtain properly folded scDR1 $\alpha\beta$ variants with increased expression level for further protein engineering and characterization, a library of scDR1 $\alpha\beta$ variants generated by error-prone PCR was screened by flow cytometric sorting with the L243 conformational antibody. Yeast cells were

selected through three cycles of sorting after labeling with the L243 antibody followed by biotinylated-GAM IgG and streptavidin-phycoerythrin (SA-PE). In each cycle, yeast cells collected from the previous sort were cultured and protein expression was induced. A modest enrichment could be observed by the second sort and a positive population was detected clearly after the third sort.

Nineteen clones isolated from the library were screened for binding to the anti-V5 antibody and anti-DR L243, LB3.1, and Immu-357 antibodies. In contrast to the wild-type construct, the mutants showed positive population of cells with the three conformational antibodies. Representative flow cytometry histograms for one of the clones selected from the library are shown in Figure 4. To ensure the phenotype of the mutant yeast was plasmid-linked, the plasmid was rescued from the respective mutant yeast clone and transformed into fresh EBY100 cells to verify that the selected phenotype was reconstituted. In general, all selected clones showed levels of binding to antibody L234 similar to those obtained with the LB3.1 and Immu-357 antibodies.

To determine whether the peptide-binding groove of these evolved scDR1 $\alpha\beta$ variants remained empty, we used the conformation-specific KL304 antibody,³⁸ which has been recently found to bind exclusively to empty MHC class II molecules.³⁹ Flow cytometric analysis of yeast cells displaying the evolved scDR1 $\alpha\beta$ variants revealed no significant binding to this antibody since only a very low percentage of cells showed some reactivity against KL304 (Figure 4). This suggested that some endogenous low affinity peptides from the yeast or peptides present in the induction media might be bound to the peptide-binding groove of the scDR1 $\alpha\beta$ molecules. Indeed, these evolved scDR1 $\alpha\beta$ variants displayed on the yeast surface were found to be associated with a collection of low-abundance peptides between 1500 and 3000 Da that could be stripped off at acidic pH and detected by matrix assisted laser desorption ionization-time of flight (MALDI-TOF) mass spectrometer (data not shown). However, as shown later, these peptides could be readily displaced

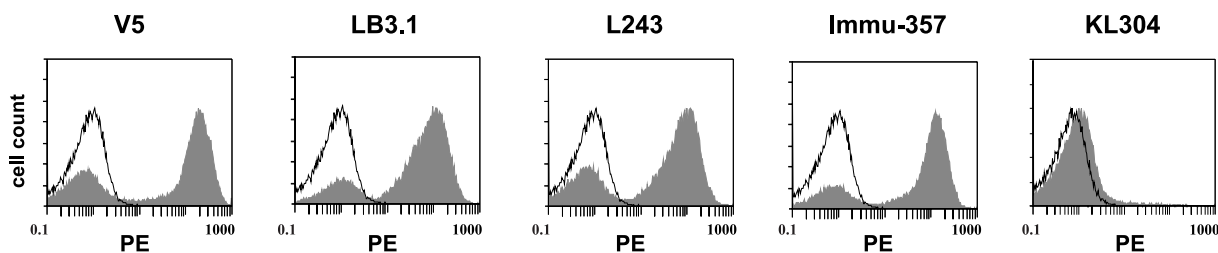


Figure 4. Flow cytometric analysis of a representative evolved scDR1 $\alpha\beta$ variant. Yeast cells displaying the mutant DWP-7 were stained with anti-V5, anti-DR L234, LB3.1, Immu-357 and anti-IA^{g,k,n,f} KL304 antibodies followed by biotinylated goat-anti-mouse IgG and SA-PE. Unshaded peaks represent yeast cells treated with only the secondary staining reagents. Labeled yeast cells were analyzed on a Coulter Epics XL flow cytometer collecting 30,000 cells gated on light scatter (size) to prevent analysis of the clumps.

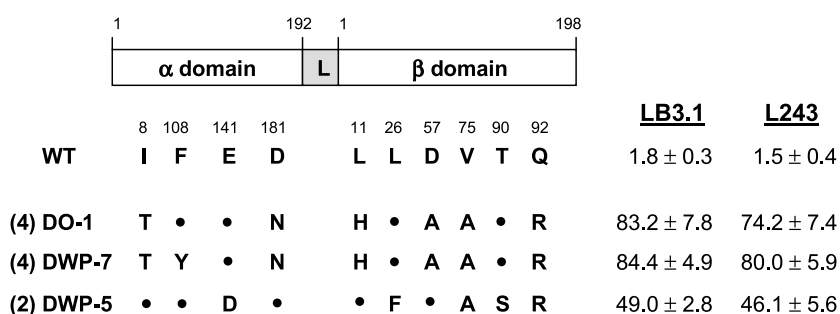


Figure 5. Sequence analysis of the evolved scDR1αβ variants. Schematic representation of the scDR1αβ construct is shown on the top of the group of sequences. The numbers below the diagram refer to amino acid positions in the α and β-chains, respectively. The number of independent isolates of each clone is shown in parentheses. The MFU values for LB3.1 and L234 antibodies are shown on the right of each sequence. Dot indicates residue is same as wild-type DR1.

The mutation L11βH was found in all the evolved variants selected of a library of single-chain DR1 molecules with the covalently bound antigenic peptide HA₃₀₆₋₃₁₈ (O.E. & H.Z., unpublished results).

by higher affinity peptides in a binding assay. Thus, it may be concluded that these evolved scDR1αβ variants are “functionally empty” rather than “physically empty”, as was previously described for other recombinant class II molecules.⁴⁰

Sequence analysis of the evolved scDR1αβ variants

Ten clones that exhibited the highest binding to the conformational antibodies LB3.1, L243 and Immu-357 were selected for sequence analysis, and were classified into three unique groups, including DO-1, DWP-7 and DWP-5 according to their sequences (Figure 5). Clones DO-1 and DWP-7 only differed in one amino acid substitution in the α-chain. Each of these variants contained multiple amino acid substitutions relative to the wild-type. It should be noted that the Lβ11H substitution was found in eight of these ten sequenced clones, and more importantly, found in all functional mutants selected from a library expressing the heterotrimer of peptide HA, β-chain and α-chain as a covalently linked single-chain protein (scHADR1βα) (O.E. & H.Z., unpublished results).

Peptide binding to the evolved scDR1αβ variants by flow cytometry assays

To determine whether the evolved scDR1αβ variants were capable of binding specific antigenic peptides, biotinylated DR-specific HA₃₀₆₋₃₁₈ peptide was used to examine its direct binding to the scDR1αβ molecules displayed on yeast cells. Binding was measured by SA-PE and flow cytometry. Figure 6 shows the histograms of fluorescence intensities of yeast displaying these evolved scDR1 variants after incubation with the biotinylated peptide for 20 hours at 37 °C. In all cases, 25 μM of biotinylated HA₃₀₆₋₃₁₈ peptide stained 100% of the cells expressing folded scDR1αβ molecules (>70% of the total yeast cells). The same result was obtained when these yeast cells displaying scDR1 had been stored at 4 °C for at least four months. In comparison, the same concentration of Tax-8Kbio, a biotinylated derivative of the peptide Tax specific for HLA-A2 molecules, resulted in fluorescence intensity similar to the background (Figure 6). Analogously, incubation of yeast cells displaying a class I MHC molecule failed to react with HA₃₀₆₋₃₁₈ peptide. HA₃₀₆₋₃₁₈ peptide bound in a dose-dependent manner with saturation at 50 μM (Figure 7(A)). Moreover, the

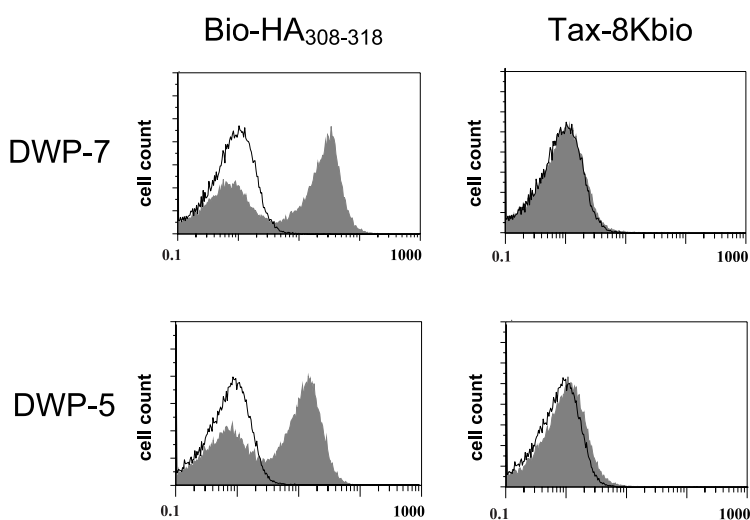


Figure 6. Flow cytometric analysis of binding of scDR1αβ variants to biotinylated HA₃₀₆₋₃₁₈ (HLA-DR1-specific) or Tax (HLA-A2-specific) peptide. (Top) The DWP-7 variant; (bottom) the DWP-5 variant. Unshaded peaks represent yeast cells treated with only the secondary staining reagents. Labeled yeast cells were analyzed on a Coulter Epics XL flow cytometer collecting 30,000 cells gated on light scatter (size) to prevent analysis of the clumps.

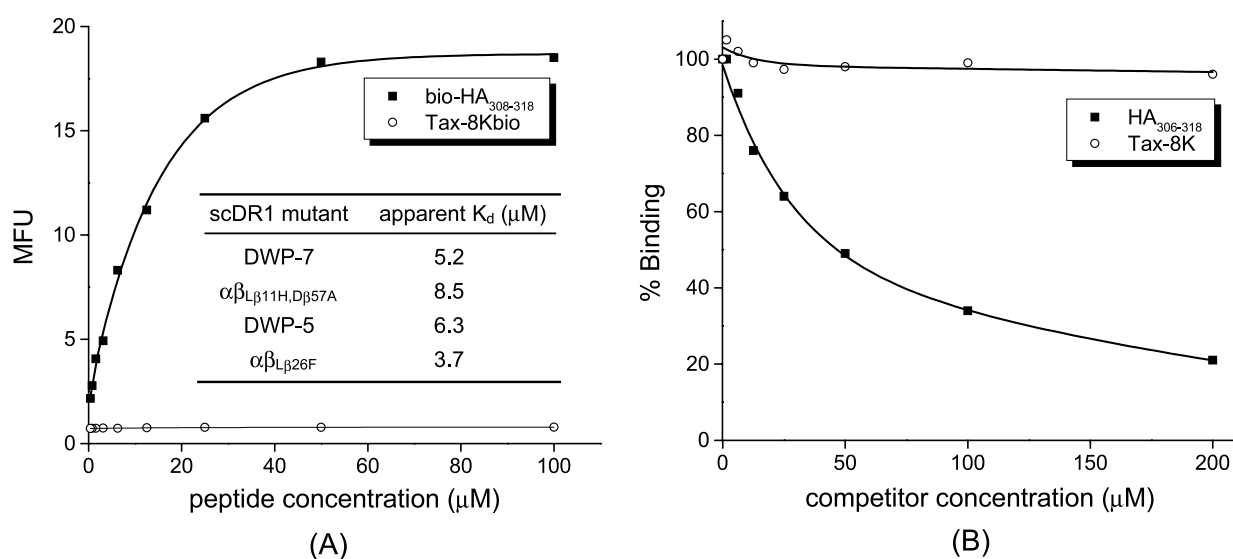


Figure 7. Specificity of peptide binding. (A) Direct peptide binding. scDR1 $\alpha\beta$ -displaying yeast cells were incubated for 20 hours at 37 °C with a series of concentrations of biotinylated DR-specific HA_{306–318} (squares) or A2-specific Tax-8K (circles) peptides. Inset: Apparent association constants of biotinylated HA_{306–318} peptide to yeast-displayed single-chain HLA-DR1 variants. (B) Competitive peptide binding. Binding of the biotinylated HA_{306–318} peptide was inhibited by an excess of the unlabeled HA_{306–318} peptide (squares), but not by an A2-specific Tax-8K peptide (circles). scDR1 $\alpha\beta$ -displaying yeast cells were incubated for 20 hours at 37 °C with 10 μM of biotinylated peptide at pH 6.5 in the presence of a competitor unlabeled peptide (0–200 μM). DR1-bound biotinylated peptide was quantified by flow cytometry. Specific binding is expressed as the percentage of binding by using the following formula: percentage of binding = [(MFU with competitor – background)/(MFU without competitor – background)] \times 100%.

binding could be blocked by an excess of unbiotinylated HA_{306–318} but not by the unlabeled Tax-8K peptide (Figure 7(B)), indicating the labeled peptide bound to the same site as the unbiotinylated natural determinant. Scatchard plots of the

binding data were linear, allowing the calculation of apparent K_d values of HA_{306–318} to DR1-displayed yeast cells (inset of Figure 7(A)).

Kinetics of peptide binding to the evolved scDR1 $\alpha\beta$ variants on yeast cell surface

The time-course of peptide binding was measured by incubation of biotinylated HA_{306–318} and the evolved scDR1 $\alpha\beta$ variants displayed on yeast cell surface for various time intervals at 37 °C (Figure 8). In contrast to the previously reported binding of HA_{306–318} to intact antigen presentation cells (APC),⁴¹ the kinetics of binding with scDR1 $\alpha\beta$ molecules were much faster and a much larger fraction of the molecules were loaded (50% maximum binding after less than five hours with a plateau after 20–24 hours), with no apparent interference from the endogenous peptides. In addition, once it formed a complex with the yeast displayed scDR1 $\alpha\beta$ variants in five hours, the HA peptide remained bound even after incubation at 37 °C for two days in the presence of an excess of unlabeled peptide (data not shown).

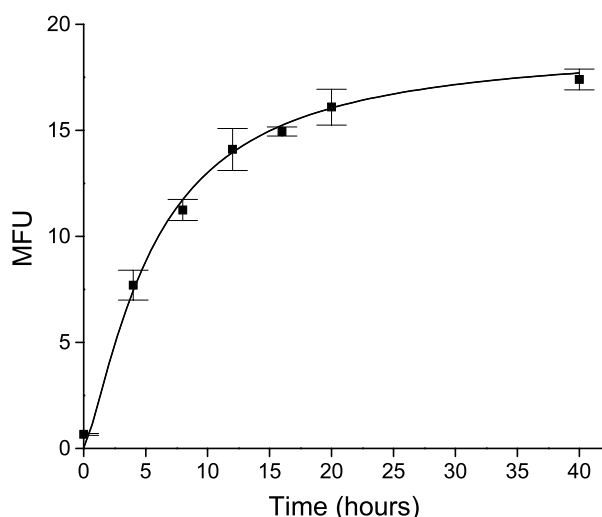


Figure 8. Kinetics of peptide binding. Association kinetics of peptide binding to yeast cells displaying mutant scDR1 $\alpha\beta_{L\beta11H,D\beta57A}$. scDR1 $\alpha\beta$ -displaying yeast cells were incubated with 40 μM of biotinylated HA_{306–318} peptide at 37 °C for different periods of time, the amount of DR1-bound peptide was examined by flow cytometry using SA-PE. Yeast-displayed scDR1 $\alpha\beta$ molecules were rapidly loaded (50% maximum signal in less than five hours and 100% in 20–24 hours).

Thermostability analysis of the evolved scDR1 $\alpha\beta$ variants

The thermal stability of the evolved scDR1 $\alpha\beta$ variants displayed on the yeast cell surface was determined as described.⁴² Since the yeast display scaffold remains intact at temperatures up to 90 °C,⁴² yeast cells that expressed different scDR1

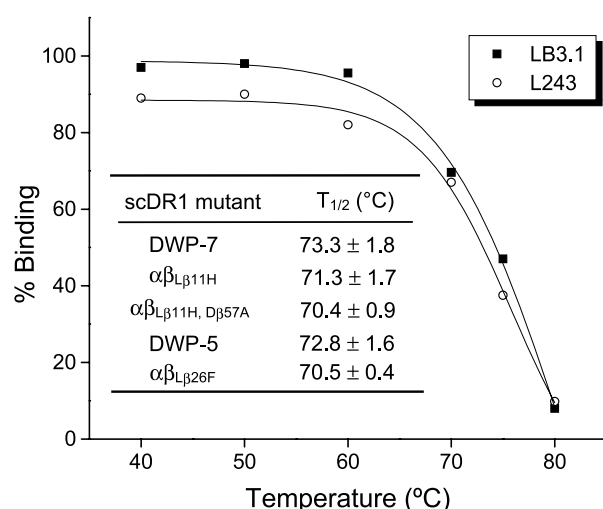


Figure 9. Irreversible denaturation curves for the DWP-7 variant displayed on the yeast cell surface. After ten minutes of incubation at the specified temperature, yeast cells were stained with conformation-sensitive DR-specific L243 and LB3.1 antibodies to monitor the fraction of native scDR1 $\alpha\beta$ remaining on the cell surface. The data points representing the mean PE fluorescence minus the autofluorescence at each temperature were fitted to a simple exponential decay curve. Representative curves of two independent titrations are presented for each antibody. The midpoint of thermal denaturation for different scDR1 $\alpha\beta$ variants obtained with L243 antibody is summarized in the inset. Similar results were obtained when LB3.1 antibody was used (the maximal difference of the calculated $T_{1/2}$ values between L243 and LB3.1 antibodies was 1.6 deg. C).

molecules were incubated at a range of temperatures below 90 °C and the fraction of active molecules was quantified by binding with two different conformational antibodies. The percentage of maximal binding was plotted with respect to temperature and used to determine the temperature at which half-maximal denaturation occurred ($T_{1/2}$) (Figure 9). The calculated $T_{1/2}$ values for scDR1 $\alpha\beta$ displayed by the different mutants were between 70.4 and 73.3 °C (inset of Figure 9). These values are near the temperature at which the secondary structure of recombinant DR1 molecules breaks down (67 °C), as determined by circular dichroism.³⁵ The functional stability of these scDR1 $\alpha\beta$ proteins was also assessed by measuring residual binding activity following incubation at 37 °C for several days. The different scDR1 $\alpha\beta$ variants displayed on yeast cells were very stable at 37 °C as revealed by the high fraction of folded proteins ($\geq 80\%$) upon incubation at 37 °C for three days.

Identification of functional mutations in the evolved scDR1 $\alpha\beta$ variants

The presence of multiple mutations in the majority of the variants makes predictions of the molecular basis for soluble expression difficult.

However, the L β 11H substitution in the β -chain was found in the majority of clones selected from a library of scDR1 $\alpha\beta$ variants (eight out of ten) and all functional clones selected from a library of scHADR1 $\beta\alpha$ variants (O.E. & H.Z., unpublished results), shedding some light on the importance of this amino acid substitution. Indeed, the presence of this single mutation in both scDR1 $\alpha\beta$ ($\alpha\beta_{L\beta11H}$) and scDR1 $\beta\alpha$ ($\beta\alpha_{L\beta11H}$) yielded a folded protein (Figure 10A). However, this single mutant showed a lower level of folded protein than the mutant DWP-7, as measured by reactivity with L243 and LB3.1 antibodies. Moreover, the reactivity of the L β 11H mutant with these two antibodies was also less than that for the double mutant scDR1 $\alpha\beta_{L\beta11H, D\beta57A}$, which gave an expression level of folded proteins comparable to that obtained for mutant DWP-7 (Figure 10A). The effect of the substitution D β 57A was clearly synergistic with the L β 11H mutation since the single mutant scDR1 $\alpha\beta_{D\beta57A}$ only gave about 20% of folded proteins with respect to the double mutant scDR1 $\alpha\beta_{L\beta11H, D\beta57A}$ (Figure 10A). On the other hand, for those clones with the sequence of DWP-5, the L β 26F substitution in the β -chain seemed to be critical for the functional expression of these mutant scDR1 molecules since the single mutant scDR1 $\alpha\beta_{L\beta26F}$ has an expression level of folded proteins similar to that showed by DWP-5 (Figure 10B).

Amino acid substitutions V β 75A and Q β 92R in the β -chain were present in all mutants selected from the library. However, they were also found in a high percentage of unselected clones. Their effect in expression of the scDR1 molecules was investigated using a mutant scDR1 $\alpha\beta$ with only these two amino acid substitutions. Like wild-type scDR1 $\alpha\beta$, scDR1 $\alpha\beta_{V\beta75A, Q\beta92R}$ did not show substantial reactivity against DR-specific conformational antibodies (Figure 10A).

Discussion

We have used directed evolution coupled with yeast cell surface display to engineer several single-chain HLA-DR1 variants without covalently linked peptides that are remarkably stable, well-expressed, and functionally empty. To the best of our knowledge, these DR1 molecules represent the first single-chain MHC molecules that are capable of directly binding specific antigenic peptides on the yeast cell surface. Three novel single site mutations, L β 11H, D β 57A and L β 26F, in the β 1 domain, were found to be critical for the proper folding of the single-chain DR1 molecules. Availability of these variants will enable further engineering and study of functional HLA-DR1 molecules as novel therapeutic and diagnostic agents for autoimmune and infectious diseases.

Yeast is a particularly useful cell-surface expression system because it enables folding and glycosylation of expressed heterologous eukaryotic

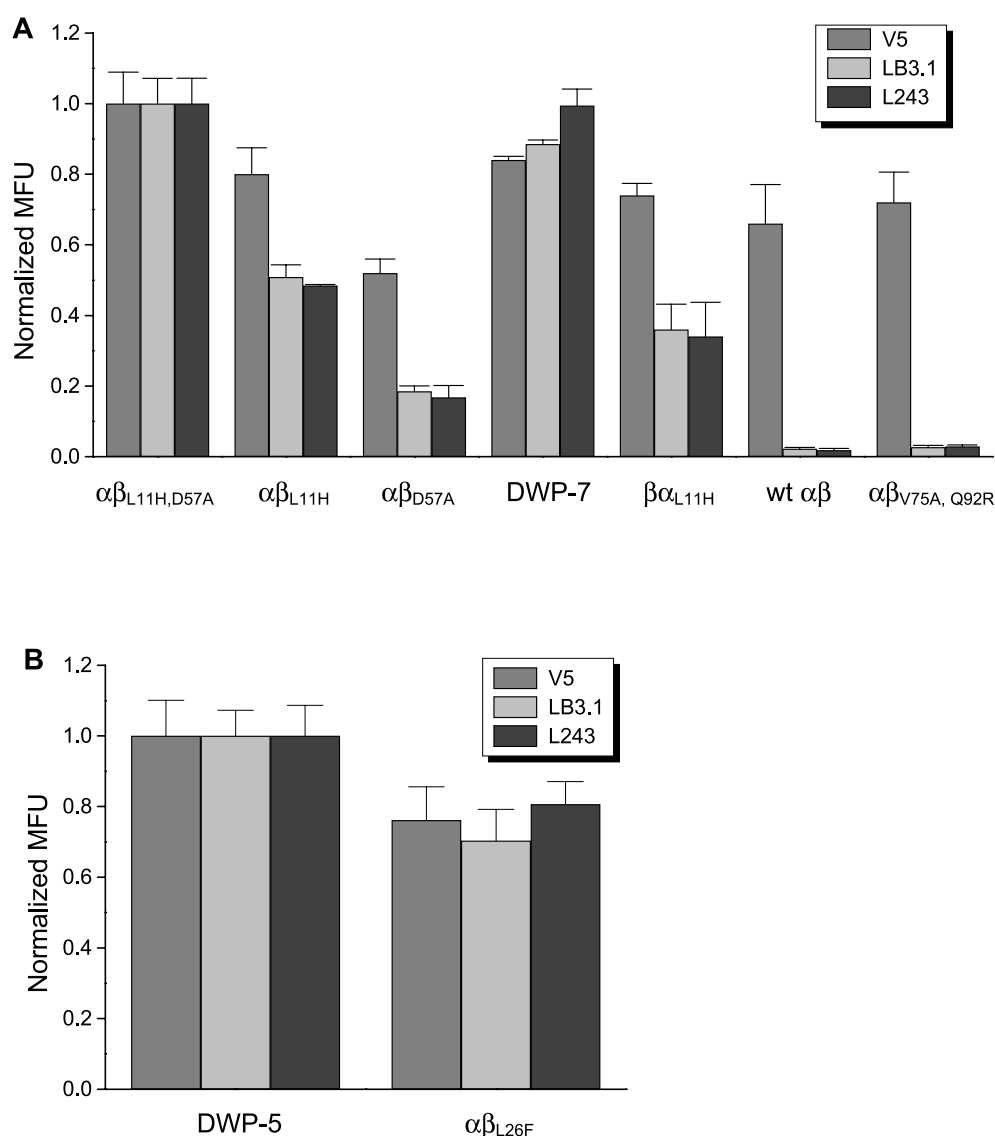


Figure 10. Identification of single site mutations in the evolved scDR1 $\alpha\beta$ variants that confer elevated expression levels of folded proteins. A, Expression levels of folded single-chain DR1 protein in different mutant yeast clones. Yeast displaying wild-type scDR1 $\alpha\beta$ are indicated as wt- $\alpha\beta$. B, Comparison of single-chain DR1 protein levels in the mutant clone LB26F with the mutant DWP-5 clone. Results are shown as background-subtracted MFU normalized to the highest MFU for each monoclonal antibody in each experiment. Error bars represent standard deviations (SDs) of three independent yeast clones.

proteins and is easy to handle with ample genetic techniques available.⁴³ However, our initial attempt to express single-chain DR1 molecules in their folded form on the yeast cell surface failed. Wild-type scDR1 $\alpha\beta$ or scDR1 $\beta\alpha$ molecules could be expressed on the yeast surface at high levels but not in their native state. This finding was unexpected since it has been reported that the quality control system of the yeast secretory apparatus allows export of only correctly folded and assembled proteins.⁴⁴ Yeast surface display of a functional single-chain DR1 molecule was achieved only after introduction of specific mutations such as L β 11H, D β 57A or L β 26F into the protein.

The effects of these mutations on soluble

expression of folded scDR1 $\alpha\beta$ molecules can be partially accounted for by molecular modeling. As shown in Figure 11A, the single-chain DR1 $\alpha\beta$ molecule consists of two polypeptide chains (α and β) connected by a 15 amino acid residue, linker. The peptide-binding groove is formed by the α 1 and β 1 domains. All these three mutations are located in the β 1 domain. Molecular modeling predicts that L β 26F mutation positions the F β 26 side-chain near those of F β 13, F β 40 and Y β 78, creating an interaction network of four aromatic residues that links three anti-parallel β -sheet strands to the α -helix within the β 1 domain (Figure 11B). Moreover, Y β 78 forms part of a conserved network of aromatic residues that appears to stabilize the secondary structure motif that is completely conserved in

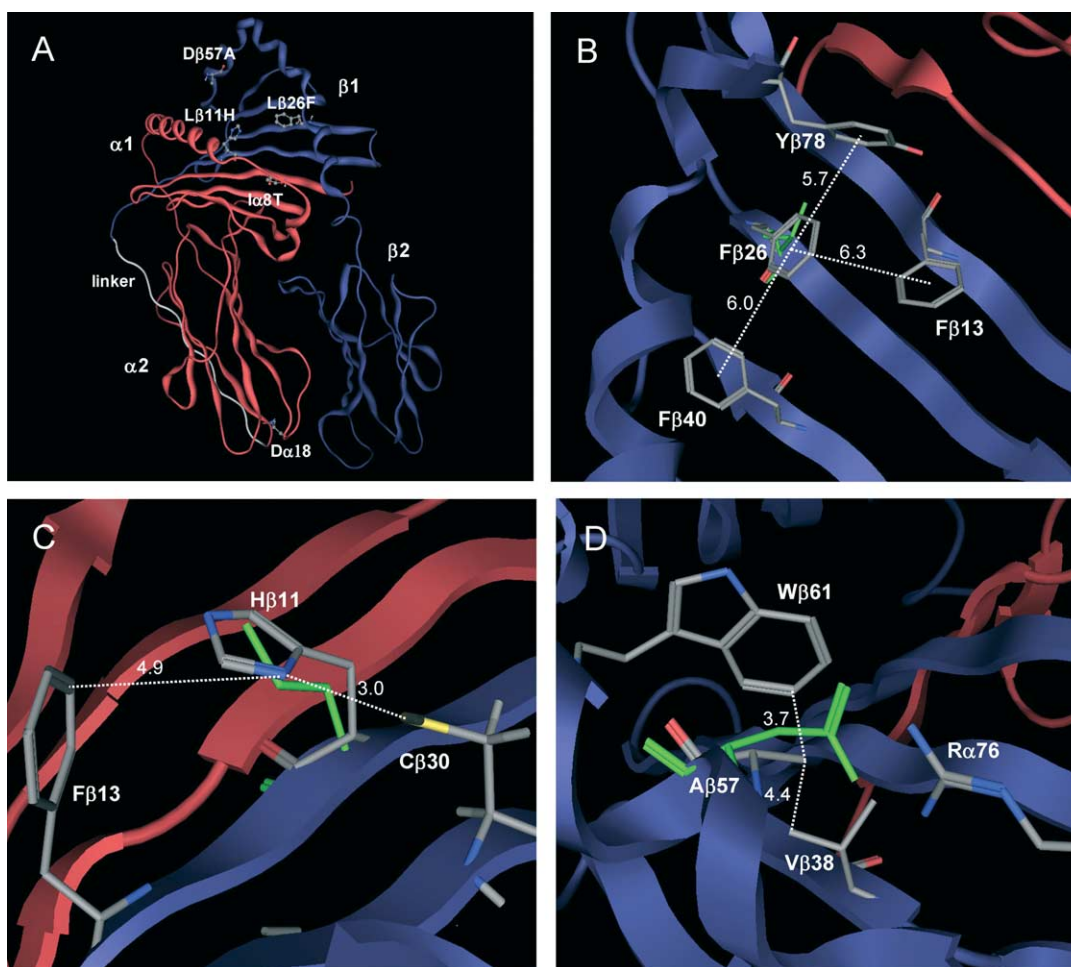


Figure 11. Molecular modeling of site-directed scDR1 $\alpha\beta$ variants. A, Schematic representation of the single-chain DR1 molecule, scDR1 $\alpha\beta$. The three mutations L β 11H, D β 57A and L β 26F important for protein folding as well as the mutations I α 8T and D α 181N found in the majority of the mutants are shown in stick-and-ball. B, The β 1 α 1 domain showing the aromatic interaction network formed by F β 26. The original L β 26 residue which is superimposed on F β 26 is shown in green. C, Region of the peptide-binding domain showing the substitution L β 11H on the β -chain. L β 11, superimposed on H β 11, is shown in green. D, Region of the β 1 α 1 domain showing the location of the mutation D β 57A. D β 57 that forms a salt bridge with R α 76 in wild-type DR1 is shown in green and appears superimposed on A β 57. The α -chain is shown in red and the β -chain is shown in blue. The broken lines indicate the distances in Å between residues forming putative hydrophobic or aromatic–aromatic interactions.

human class II molecules and is highly conserved between rat, mouse and human MHC class II molecules.⁴⁵ Therefore, F β 26 could contribute to a tighter packing of the hydrophobic core in the β 1 α 1 domain by increasing the number of aromatic–aromatic interactions and consequently to its overall stability. Indeed, far-sequence aromatic pairs have been shown to stabilize protein tertiary structures.⁴⁶ In addition, although the total contribution of aromatic–aromatic interactions to the stability of proteins may be small relative to other types of interactions, it might be important for protein folding since these interactions may form nucleation sites in the protein folding pathway.⁴⁷

The L β 11H mutation seems to play an important role in the expression of folded scDR1 $\alpha\beta$ molecules. Although position 11 in the β -chain is polymorphic, His is not found in any of the DR alleles

with known sequences. Molecular modeling indicates that the substitution L β 11H on the first β -sheet strand of the β 1 domain approaches the $\delta(+)$ amino group of H β 11 within 5 Å of the ring centroid of F β 13 where it makes van der Waals contacts with the $\delta(-)$ π -electrons of the ring (Figure 11C). This amino–aromatic interaction is analogous to the enthalpically favorable interaction between aromatic side-chains.⁴⁷ In addition, the sulfur atom of C β 30 is placed at 4 Å from the ring centroid of H β 11, and may form a strong non-covalent interaction with the π -electron system of the aromatic ring (histidine) of H β 11. Sulfur–aromatic interactions are weakly polar interactions that are stronger than van der Waals interactions between non-polar atoms.⁴⁸ These sulfur–aromatic interactions are commonly observed in the hydrophobic core of proteins and may have special

significance for stabilizing the folded conformation of proteins.^{49,50} The D β 57A mutation also promotes the folding of the single-chain DR1 $\alpha\beta$ molecule since its presence in the single mutant L β 11H increases the expression level of folded protein by up to 50% (Figure 10A). Position D β 57 in DRB alleles, although usually Asp, is polymorphic. Interestingly, the substitution D β 57A is characteristic of DQ alleles that correlate with insulin-dependent diabetes mellitus (IDDM) susceptibility.⁵¹ Residues D β 57 in the β 1 domain and R α 76 in the α 1 domain form a salt-bridge underneath the bound peptide that links the HLA-DR1 β 1 and α 1 chain helical regions. The substitution of Asp by Ala breaks this salt bridge and therefore could destabilize the structure of HLA-DR1. However, our thermostability data obtained with the mutant scDR1 $\alpha\beta$ _{L β 11H,D β 57A} (inset of Figure 9) do not seem to indicate that the D β 57A substitution affects the stability of the single-chain DR1 molecules. This observation is in agreement with data reported for DQ molecules in which the D β 57A substitution predominately alters the peptide-binding specificity rather than the overall stability of either empty or peptide-loaded forms of these MHC molecules.⁵² Therefore, the contribution of this salt bridge does not seem to be important for protein stability. However, formation of this salt bridge might be a kinetic barrier for the folding of the scDR1 $\alpha\beta$ molecule, as was proposed for other proteins.⁵³ Since A β 57 increases the hydrophobic interaction with V β 38 and W β 61 in the β 1 chain (Figure 11D), it is likely that D β 57A may lower a kinetic barrier in the folding pathway of single-chain DR1 by enhancing the stability of the hydrophobic core of the β 1 α 1 domain. However, we cannot exclude the possibility that these three mutations favor the close packing with some yeast endogenous peptides that in turn help to stabilize a conformation that is critical to subsequent binding of high affinity peptides, such as the HA_{306–318} peptide. Recently, it has been reported that mutation S11F in the β 1 domain of DR3 stabilized the CLIP peptide in the antigen-binding groove,⁵⁴ whereas different mutations in the residue 57 β of I-A⁸⁷ molecules yielded more stabilized variants.³³ Other mutations, such as I α 8T or D α 181N, seem to be not important for the folding of scDR1. As shown in Figure 11A, mutation I α 8T is located on the interface between α 1 β 1 and α 2 β 2. The single mutant $\alpha\beta$ _{I α 8T} showed near background reactivity against the conformational antibodies L243 and LB3.1 (data not shown), indicating a negligible role of this mutation in the folding of scDR1. The other mutation, D α 181N, is located on a surface-exposed loop at the carboxyl terminal end of β 2, far away from the peptide-binding platform. Thus, this mutation is also unlikely important for the folding or stability of scDR1.

The evolved single-chain DR1 variants were folded properly since they reacted with several conformation-sensitive DR-specific monoclonal

antibodies and formed a stable complex with DR-specific antigenic peptide HA_{306–318}. Although these molecules seem to be occupied by some endogenous peptides, they were fully competent to bind exogenously added peptides. Furthermore, the kinetics of the peptide binding was also much faster than those reported for human or mouse class II proteins (50% maximum binding after less than five hours) (Figure 8). More importantly, as shown in Figure 7, the binding of HA_{306–318} to these variants was specific, sensitive, and appeared in a dose-dependent manner, which provides the basis for the development of high throughput screening methods for directed evolution of DR1 variants with improved peptide binding affinity or isolation of novel DR1-binding peptides.

The apparent K_d values of these variants determined by Scatchard plots were six to 12-fold lower than that obtained for DR1 molecules on the cell surface (50 μ M) using indirect labeling and flow cytometry,⁴¹ but higher than that of purified recombinant DR1 (14 nM).⁵⁵ However, these direct binding assays do not necessarily reflect the intrinsic affinity between peptide and MHC. The measured affinities may also contain contributions from conformational changes. It was recently shown that the conformational change in the DR1 molecules is the rate-determining step for HA_{306–318} binding to DR1, indicating that the energy barrier for the conformational change is significantly higher than that for peptide binding.⁵⁶ As a result, the peptide binding affinity could be vastly underestimated. It is noteworthy that although some yeast endogenous peptides may remain bound to the scDR1 $\alpha\beta$ variants, and in turn, contribute to maintain scDR1 $\alpha\beta$ molecules in a peptide-receptive conformation, other additional conformational changes may be required for the binding of specific high-affinity peptides. The observation that scDR1 $\alpha\beta$ molecules displayed on the yeast cell surface increase their reactivity against the LB3.1 and L243 antibodies upon incubation with the HA_{306–318} peptide suggests that the binding of the high-affinity peptide HA_{306–318} further changes the conformation that is shaped by the low affinity peptides. In addition, inherent problems of cellular binding assays such as aggregation of cells or other technical difficulties such as limited solubility of peptides may complicate the measurement of the real affinities.

Yeast-displayed scDR1 $\alpha\beta$ variants formed stable $\alpha\beta$ heterodimers in the absence of an antigenic peptide (Figure 8). The “functionally empty” heterodimers remained stable after incubation at 37 °C for three days and they were capable of binding peptide after storage at 4 °C for more than four months. It has been reported that empty class II MHC molecules lose their receptive conformation quickly and consequently their ability for rapid binding of peptides.⁵⁶ Conversely, class II molecules that are bound to peptide ligand are extremely receptive for the binding of other higher affinity peptides.⁵⁶ Thus, the use of the

yeast-displayed scDR1 molecules that are dissociating from low-affinity yeast peptides may provide a homogenous pool of active MHC molecules for determination of peptide binding.

The system and strategy developed for display of functionally empty single-chain HLA-DR1 molecules may serve as a platform technology for development of new MHC-based diagnostic and therapeutic reagents. Since the binding of exogenous labeled peptides to cell surface-associated HLA-DR1 can be monitored by flow cytometry at the single cell level, this system may allow the further engineering of DR1 molecules with novel or improved peptide specificity or increased peptide affinity with great ease. Thus, these engineered DR1 molecules may exhibit better clinical performance therapeutics and diagnostics reagents for autoimmune and infectious diseases. Similarly, the system developed might also enable the design of peptide-based vaccines with improved clinical performance. In addition, since the DR-peptide binding reaction can be easily monitored by flow cytometry, the ability to engineer MHC molecules by yeast cell surface display and directed evolution may offer excellent opportunities to characterize structural requirements in peptide binding for those class II and class I molecules recalcitrant to expression or purification.⁵⁷ Finally, it was reported that proteins expressed at higher levels on the yeast cell surface are also expressed at significantly higher levels in a yeast secretion system.⁵⁸ Indeed, mutant scDR1 $\alpha\beta$ _{L β 11H,D β 57A} resulted in more soluble folded proteins than the wild-type scDR1 $\alpha\beta$ when expressed in *Saccharomyces cerevisiae* BJ5464 (O.E. & H.Z., unpublished results). Thus, it may now be possible to produce selected class II proteins at a large scale in yeast secretion systems that have not been successful to date.

Materials and Methods

Materials

sscDR β HA plasmid⁵⁹ that encodes the single-chain HA $\beta\alpha$ gene was provided by Dr M. Mage (NIH, Bethesda, MD) and served as a template for PCR cloning. pYD1, a vector for yeast surface display of proteins, and *S. cerevisiae* EBY100 strain were purchased from Invitrogen (Carlsbad, CA). Oligonucleotides were synthesized by Integrated DNA Technologies (Coralville, IA). Cloned *PfuTurbo* DNA polymerase and *Escherichia coli* XL1-Blue were purchased from Stratagene (La Jolla, CA). *Taq* DNA polymerase was purchased from Promega (Madison, WI). Endonuclease restriction enzymes, DNA ligase and PNGase were from New England Biolabs (NEB, Beverly, MA). Peptides used here were synthesized and purified (>90%) commercially (Jerini AG, Berlin, Germany) and included a peptide containing residues 306–318 of influenza virus hemagglutinin (HA_{306–318}) and a HLA-A2-specific Tax-derivative peptide (Tax-8K). For biotinylated HA_{306–318} peptide (bio-HA_{306–318}), the biotin was attached to its N terminus *via* a linker of two 6-amino-hexanoic acid molecules. For biotinylated Tax peptide, the biotin was attached to the

ϵ -amino group of a lysine residue, substituted at position 8 of the Tax peptide (Tax-8Kbio). Monoclonal antibodies used here were anti-DR L243 (Biodesign International, Saco, ME), LB3.1 (American Tissue Culture Collection (ATCC), Manassas, VA), Immu-357 (Beckman Coulter, Fullerton, CA), anti-DR, -DP and -DQ CR3/43 (Biomedica, Foster City, CA), anti-IA^{s,k,u,f} KL304 (ATCC), anti-Xpress, and anti-V5 (Invitrogen, Carlsbad, CA). Biotin-conjugated goat-anti-mouse (GAM) IgG was purchased from Rockland (Gilbertsville, PA) and streptavidin-phycoerythrin (SA-PE) conjugate was purchased from PharMingen (San Diego, CA). Alkaline phosphatase-conjugated GAM IgG was purchased from Sigma (St. Louis, MO). The Zymoprep miniprep kit was obtained from ZymoResearch (Orange, CA). The QIAprep spin plasmid mini-prep kits and QIAquick PCR purification kits were purchased from Qiagen (Valencia, CA). Unless otherwise indicated, all chemicals were purchased from Sigma (St. Louis, MO).

Generation of single-chain DR1 constructs

DNA encoding the extracellular domains of DR α and DR β joined by a linker of 15 amino acid residues (G₄SG₃-RSG₅) (scDR1 $\alpha\beta$) was prepared by splicing overlap extension PCR (SOE-PCR).⁶⁰ The α and β -domains were amplified from plasmid sscDR β HA with the oligonucleotide pairs α -5BX (5' GTACCAGGATCCAGTG TGGTGGAAAGGAAAGAACATGTGATC 3')/ α -3GS (5' GCCAGAGCGGCCGCCACCTGAGCCGCCCGCTCTACGTTCTCTGTAGTCTCTGG 3'), and β -5GS (5' TCAG GTGGCGGCCGCTCTGGCGGAGGTGGATCCGGGGA CACCCGACCAC 3')/ β -3XH (5' CCCTCTAGACTCG AGCTTGCTCTGTGCAGATTCAGAC 3'), respectively. The primers α -3GS and β -5GS overlap by 20 nucleotides (nt) and were modified to introduce a unique NotI restriction site in the linker sequence that connects the α to the β -domain. These two PCR products were mixed together and assembled by a primerless PCR, followed by reamplification of the assembled products with the external oligonucleotides α -5BX and β -3XH. The final product was purified, digested with BstXI and XhoI and cloned into the pYD1 vector digested with the same restriction enzymes, giving the plasmid pYD1sc $\alpha\beta$ (Figure 1). DNA encoding the single-chain $\beta\alpha$ (scDR1 $\beta\alpha$) was also obtained from plasmid sscDR β HA by PCR amplification with the oligonucleotides β -5BX (5' GTAC CAGGATCCAGTGTGGTGGAAAGGGGACACCCGACC ACG 3') and α -3XH (5' CCCTCTAGACTCGAGTAAGT TCTC TGTA GTCTCTGG 3'). The resulting amplification product was cloned into pYD1 *via* BstXI and XhoI to give pYD1sc $\beta\alpha$ (Figure 1). The plasmids were sequenced through the entire encoding sequence to verify the absence of undesired mutations introduced by PCR.

Site-directed mutagenesis

Plasmids pYD1sc $\alpha\beta$ _{L β 11H}, pYD1sc $\alpha\beta$ _{L β 26F}, pYD1sc $\alpha\beta$ _{L β 11H,D β 57A}, pYD1sc $\alpha\beta$ _{D β 57A}, pYD1sc $\alpha\beta$ _{V β 75A,Q β 92R} and pYD1sc β _{L β 11H} α were constructed using yeast *in vivo* recombination.^{61,62} For construction of pYD1sc $\alpha\beta$ _{L β 11H} encoding scDR1 $\alpha\beta$ with the mutation L β 11H in the β -chain, a DNA fragment encoding the last eight amino acid residues at the carboxyl terminus of the α -chain, the linker region, and the first 56 amino acid residues of the β -chain were amplified with primers α _{for183} (5' CCAAG CCCTCTCCCAGAGAC 3') and β _{rev56} (5' GGCC GCCCAGCTCC 3') by cloned *PfuTurbo* polymerase

using the DO-1 mutant as a template. The resulting PCR fragment was cotransformed into *S. cerevisiae* EBY100 strain with the NotI-cut pYD1 $\alpha\beta$ DNA. Gap-repair by *in vivo* yeast homologous recombination yielded plasmid pYD1sc $\alpha\beta_{L\beta11H}$. Similarly, for construction of pYD1sc $\alpha\beta_{L\beta11H, D\beta57A}$, a DNA fragment encoding the last eight amino acid residues at the carboxyl terminus of the α -chain, the linker region, and the first 73 amino acid residues of the β -chain were amplified with primers α_{for183} and $\beta_{rev73-67}$ (5' GGCCCGCCTCTGCTCCAGGA 3') using the DO-1 mutant as a template and inserted into the NotI-cut pYD1 $\alpha\beta$ by yeast homologous recombination. pYD1sc $\alpha\beta_{L\beta26F}$ was constructed in the same way except that PCR was conducted using DWP-5 as a template. pYD1sc $\alpha\beta_{D\beta57A}$ was obtained by cotransformation of EBY100 with the NotI-cut pYD1 $\alpha\beta_{L\beta11H, D\beta57A}$ DNA and the PCR fragment encoding the linker region and the first 55 amino acid residues of the β -chain of the wild-type scDR1 $\alpha\beta$. Yeast EBY100 clones with plasmids containing the desired mutations were selected by PCR screening with specific primers.

The PCR product encoding the single-chain $\alpha\beta$ with the mutations V β 75A and Q β 92R was also obtained by SOE-PCR. Briefly, DNA encoding the carboxyl terminal half of the α -chain, the linker, and the first 73 amino acid residues from the β -chain were amplified from pYD1sc $\alpha\beta$ with primers α -back (5' CATAGCTGTGGAC A AAGC 3') and $\beta_{rev73-67}$. DNA encoding amino acid residues 67 to 196 from the β -chain was amplified from the DO-1 mutant with primers $\beta_{for67-73}$ (5' TCCTGGAGCAG AGGCGGGCC 3') and pYDR3 (5' AGTATGTGTAAGT TGTAACG 3'). Primers $\beta_{rev73-67}$ and $\beta_{for67-73}$ overlap 20 nt at their 5' end to force the annealing of the two resulting PCR fragments during the SOE-PCR reaction. After primerless PCR assembly and reamplification with primers α -back and pYDR3, the DNA fragment was cloned into NotI/XhoI cut pYD1sc $\alpha\beta$ by yeast homologous recombination to give pYD1sc $\alpha\beta_{V\beta75A, Q\beta92R}$.

For construction of pYD1sc $\beta_{L\beta11H}\alpha$, DNA encoding sc $\beta\alpha$ with the mutation L β 11H in the β -chain was amplified from plasmid H2-1 with primers Xpress (5' GGTCC GGATCTGTACGACGATGACGATAAGGTACCAGGAT CCAGTGGGGACACCCGACCACGTTTC 3') and α -3XH in the presence of cloned *PfuTurbo* DNA polymerase. pYD1sc $\beta_{L\beta11H}\alpha$ was finally obtained by recombining the overlapping PCR fragment into BstXI/SpeI digested pYD1sc $\beta\alpha$ through cotransformation of both DNA molecules in *S. cerevisiae* EBY100 strain.

Plasmids of the different site-directed mutants were rescued from yeast cells, transferred into *E. coli*, and sequenced to confirm the presence of the introduced specific mutations and the absence of PCR associated random mutations.

Generation of a library of scDR1 $\alpha\beta$ variants

Error-prone PCR was used to create a library of scDR1 $\alpha\beta$ variants as described elsewhere.⁶³ Briefly, the scDR1 $\alpha\beta$ construct was amplified from pYD1sc $\alpha\beta$ using a flanking AGA2-specific upstream primer, pYD1for (5' AGTAACGTTTGTCTAGTAATTGC 3'), and a MAT α transcription terminator-specific downstream primer, pYDR3. The purified PCR product was digested with BstXI and XhoI and ligated into BstXI-XhoI-digested pYD1. The ligation mixture was transformed into XL-Blue electrocompetent *E. coli* yielding a library of 1.1×10^6 transformants. Clones of the library were pooled into 400 ml LB supplemented with

ampicillin and tetracycline, and grown overnight at 37°C. Plasmid DNA was purified and transformed into yeast strain EBY100 as described elsewhere.⁶⁴

Protein expression and analysis

EBY100 clones harboring the single-chain DR1 molecules were grown in SD-CAA (4% (w/v) dextrose, 0.67% (w/v) yeast nitrogen base, 1% (w/v) Casamino acids) at 30°C for ≈ 20 hours. To induce AGA2 fusion protein expression, yeast cells were centrifuged and suspended to an absorbance value of $A_{600} \approx 1.0$ in SG-CAA (2% (w/v) galactose, 0.67% yeast nitrogen base, 1% Casamino acids) (for induction of libraries) or YPG medium (10 g/l yeast extract, 20 g/l peptone, 20 g/l galactose) (for induction of individual clones) at 20°C for 48 hours. For immunoblot analysis, 5×10^7 cells were centrifuged and resuspended in 50 μ l of sample buffer (0.06 M Tris-HCl (pH 6.8), 10% (v/v) glycerol, 2% (w/w) SDS, 5% (v/v) 2-mercaptoethanol and 0.0025% bromophenol blue) and boiled for five minutes. Ten microliters of this sample was taken for analysis by SDS-12% PAGE and electrotransferred onto PVDF membranes. After blocking with bovine serum albumin (BSA), the membrane was subjected to immunodetection with the DR, DP and DQ β -chain-specific antibody CR3/43 for one hour at room temperature. Alkaline phosphatase-conjugated GAM antibody was used as a secondary antibody. The membranes were finally developed with the chromogenic substrates bromo-4-chloro-3-indolyl-phosphate and nitroblue tetrazolium. For flow cytometric analysis, $\approx 10^7$ cells were washed with phosphate buffered saline (PBS) containing 0.5% (w/v) BSA and incubated for one hour at 4°C with the primary antibody staining reagent. The antibodies used were anti-DR L243, LB3.1, Immu-357, CR3/43; anti-IA^{s,k,u,f} KL304, anti-V5, and anti-Xpress. Cells were washed with PBS containing 0.5% BSA and incubated for one hour at 4°C with biotinylated GAM IgG followed by SA-PE for 30 minutes at 4°C. Labeled yeast cells were analyzed on a Coulter Epics XL flow cytometer at the Biotechnology Center of University of Illinois (Urbana, IL).

Selection of scDR1 $\alpha\beta$ variants by fluorescence activated cell sorting (FACS)

The library of scDR1 $\alpha\beta$ variants was sorted through three cycles of FACS after yeast cell staining with anti-HLA-DR antibody L243 followed by biotin-labeled GAM IgG and SA-PE conjugate. In each cycle, yeast cells collected from the previous sort were cultured in SD-CAA and protein expression was induced with SG-CAA as described in the previous section. A total of 5×10^7 cells were examined during the first sorting round and $\approx 1.5\%$ of the population with the highest fluorescence were collected by using a Coulter 753 bench fluorescence-activated cell sorter. 10^7 cells were screened during the second and third sorting round and the top 0.4% and 0.1% of the population were collected, respectively. The concentrations of L243 antibody used for staining were 4 μ g/ml for the first two sorts and 0.4 μ g/ml for the third sort. After the third round, sorted cells were plated on selective media and individual clones were isolated and analyzed by flow cytometry with the conformational antibodies L243, LB3.1 and Immu-357 as well as the anti-V5 antibody. Plasmids of those clones with the highest fluorescence were rescued from yeast using a Zymoprep miniprep kit and

transformed into *E. coli* DH5 α cells. Plasmids were purified using a Qiaprep spin plasmid miniprep kit. DNA sequencing was carried out using a BigDye™ sequencing kit and an ABI PRISM 3700® sequencer (Applied Biosystems, Foster City, CA) at the Biotechnology Center of University of Illinois (Urbana, IL).

Peptide binding assay

4×10^6 yeast cells expressing single-chain DR1 molecules were incubated with biotinylated HA_{306–318} (HLA-DR1-specific) or Tax (HLA-A2-specific) peptide at various concentrations for 20 hours at 37 °C in 40 μ l of YPG (pH 6.5). Cells were then washed and stained with SA-PE for one hour at 4 °C and analyzed by flow cytometry. Yeast cells displaying class I molecules were also used as a negative control. For competitive binding assays, the biotinylated HA_{306–318} peptide at a final concentration of 10 μ M in 50 μ l of YPG was incubated with different concentrations of unlabeled competitors (HA_{306–318} or Tax-8K) and 4×10^6 scDR1-displaying yeast cells for 20 hours at 37 °C.

To determine the kinetics of peptide binding, 4×10^6 yeast cells displaying scDR1 $\alpha\beta$ molecules were incubated with 40 μ M of biotinylated HA_{306–318} at 37 °C for different time intervals and the fraction of bound peptide was measured with SA-PE as described above.

Thermal stability assay

The thermal stability of scDR1 $\alpha\beta$ variants was monitored directly on the yeast cell surface as described elsewhere.⁴² Samples of 4×10^6 yeast cells were incubated at temperatures of 40, 50, 60, 70, 75 or 80 °C for ten minutes. Immediately after the incubation period, protein denaturation was halted with ice-cold PBS containing 0.5% BSA. Yeast cells were centrifuged and the fraction of folded DR1 protein was determined by incubation with conformation-sensitive L234 and LB3.1 antibodies followed by biotinylated-labeled goat-anti-mouse and SA-PE. Thermal denaturation curves were generated in two independent experiments and the $T_{1/2}$ values (temperature at which half-maximal denaturation occurred) were calculated.

Molecular modeling

The crystal structure of the human class II DR1 in complex with the HA_{306–318} peptide⁶⁵ (Protein Data Bank accession code: 1DLH) was used as the basis for molecular modeling by the Molecular Operating Environment (MOE; Chemical Computing Groups Inc., Montreal, Canada). A rotamer search was performed with the single site specific mutation (L β 11H, D β 57A or L β 26F) and the whole structures of the single mutant (L β 26F) and the double mutant (L β 11H and D β 57A) were energy minimized with the bound peptide. Energy minimization was performed using the MMFF94 forcefield. To facilitate the examination of the molecular basis of these mutations on the proper folding of evolved scDR1 $\alpha\beta$ variants, the three-dimensional structures of the modeled single scDR1 $\alpha\beta$ mutants and the wild-type DR1 in complex with HA_{306–318} were superimposed.

Acknowledgements

We thank Dr Michael Mage for providing us the sscDR β HA plasmid, Dr Jeffrey Frelinger for the KL295 monoclonal antibody that was used in substitution for the KL304 antibody in our early experiments, and Dr Dave Kranz and his group members, especially Brent Orr & Susan Brophy, for helpful discussions and advice on the yeast display system. We also thank the School of Chemical Sciences' Computer Application and Network Services (CANS) group at University of Illinois for access to MOE and Barbara Pilas, Ben Montez & Igor Trilisky of University of Illinois Flow Cytometry Facility for flow cytometry and FACS assistance. The authors are grateful for comments on the manuscript by Dr Dave Kranz. This work was supported by the Campus Research Board and the Department of Chemical and Biomolecular Engineering of University of Illinois at Urbana-Champaign.

References

1. Strominger, J. L. & Wiley, D. C. (1995). The 1995 Albert Lasker Medical Research Award. The class I and class II proteins of the human major histocompatibility complex. *J. Am. Med. Assoc.* **274**, 1074–1076.
2. Tiwari, J. L. & Terasaki, P. I. (1981). HLA-DR and disease associations. *Prog. Clin. Biol. Res.* **58**, 151–163.
3. Singh, N., Agrawal, S. & Rastogi, A. K. (1997). Infectious diseases and immunity: special reference to major histocompatibility complex. *Emerging Infect. Dis.* **3**, 41–49.
4. Maile, R., Wang, B., Schooler, W., Meyer, A., Collins, E. J. & Frelinger, J. A. (2001). Antigen-specific modulation of an immune response by *in vivo* administration of soluble MHC class I tetramers. *J. Immunol.* **167**, 3708–3714.
5. Casares, S., Hurtado, A., McEvoy, R. C., Sarukhan, A., von Boehmer, H. & Brumeanu, T. D. (2002). Down-regulation of diabetogenic CD4 + T cells by a soluble dimeric peptide-MHC class II chimera. *Nature Immunol.* **3**, 383–391.
6. Masteller, E. L., Warner, M. R., Ferlin, W., Judkowski, V., Wilson, D., Glaichenhaus, N. & Bluestone, J. A. (2003). Peptide-MHC class II dimers as therapeutics to modulate antigen-specific T cell responses in autoimmune diabetes. *J. Immunol.* **171**, 5587–5595.
7. Sharma, S. D., Nag, B., Su, X. M., Green, D., Spack, E., Clark, B. R. & Sriram, S. (1991). Antigen-specific therapy of experimental allergic encephalomyelitis by soluble class II major histocompatibility complex-peptide complexes. *Proc. Natl Acad. Sci. USA*, **88**, 11465–11469.
8. Kwok, W. W., Ptacek, N. A., Liu, A. W. & Buckner, J. H. (2002). Use of class II tetramers for identification of CD4 + T cells. *J. Immunol. Methods*, **268**, 71–81.
9. Boehncke, W. H., Takeshita, T., Pendleton, C. D., Houghten, R. A., Sadegh-Nasseri, S., Racioppi, L. *et al.* (1993). The importance of dominant negative effects of amino acid side chain substitution in peptide-MHC molecule interactions and T cell recognition. *J. Immunol.* **150**, 331–341.
10. van der Burg, S. H., Visseren, M. J., Brandt, R. M.,

- Kast, W. M. & Melief, C. J. (1996). Immunogenicity of peptides bound to MHC class I molecules depends on the MHC-peptide complex stability. *J. Immunol.* **156**, 3308–3314.
11. Hackett, C. J. & Sharma, O. K. (2002). Frontiers in peptide-MHC class II multimer technology. *Nature Immunol.* **3**, 887–889.
 12. Arnold, F. H. (2001). Combinatorial and computational challenges for biocatalyst design. *Nature*, **409**, 253–257.
 13. Schmidt-Dannert, C. (2001). Directed evolution of single proteins, metabolic pathways, and viruses. *Biochemistry*, **40**, 13125–13136.
 14. Waldo, G. S. (2003). Genetic screens and directed evolution for protein solubility. *Curr. Opin. Chem. Biol.* **7**, 33–38.
 15. Pedelacq, J. D., Piltch, E., Liong, E. C., Berendzen, J., Kim, C. Y., Rho, B. S. *et al.* (2002). Engineering soluble proteins for structural genomics. *Nature Biotechnol.* **20**, 927–932.
 16. Bulter, T., Alcalde, M., Sieber, V., Meinhold, P., Schlachtbauer, C. & Arnold, F. H. (2003). Functional expression of a fungal laccase in *Saccharomyces cerevisiae* by directed evolution. *Appl. Environ. Microbiol.* **69**, 987–995.
 17. Kalandadze, A., Galleno, M., Foncerrada, L., Strominger, J. L. & Wucherpfennig, K. W. (1996). Expression of recombinant HLA-DR2 molecules—replacement of the hydrophobic transmembrane region by a leucine zipper dimerization motif allows the assembly and secretion of soluble DR alpha beta heterodimers. *J. Biol. Chem.* **271**, 20156–20162.
 18. Scott, C. A., Garcia, K. C., Carbone, F. R., Wilson, I. A. & Teyton, L. (1996). Role of chain pairing for the production of functional soluble IA major histocompatibility complex class II molecules. *J. Expt. Med.* **183**, 2087–2095.
 19. Kozono, H., White, J., Clements, J., Marrack, P. & Kappler, J. (1994). Production of soluble MHC class II proteins with covalently bound single peptides. *Nature*, **369**, 151–154.
 20. Scheirle, A., Takacs, B., Kremer, L., Marin, F. & Sinigaglia, F. (1992). Peptide binding to soluble HLA-DR4 molecules produced by insect cells. *J. Immunol.* **149**, 1994–1999.
 21. Stern, L. J. & Wiley, D. C. (1992). The human class II MHC protein HLA-DR1 assembles as empty alpha beta heterodimers in the absence of antigenic peptide. *Cell*, **68**, 465–477.
 22. Boder, E. T. & Wittrup, K. D. (1997). Yeast surface display for screening combinatorial polypeptide libraries. *Nature Biotechnol.* **15**, 553–557.
 23. Boder, E. T. & Wittrup, K. D. (1998). Optimal screening of surface-displayed polypeptide libraries. *Biotechnol. Prog.* **14**, 55–62.
 24. Yeung, Y. A. & Wittrup, K. D. (2002). Quantitative screening of yeast surface-displayed polypeptide libraries by magnetic bead capture. *Biotechnol. Prog.* **18**, 212–220.
 25. Wittrup, K. D. (2001). Protein engineering by cell-surface display. *Curr. Opin. Biotechnol.* **12**, 395–399.
 26. Boder, E. T., Midelfort, K. S. & Wittrup, K. D. (2000). Directed evolution of antibody fragments with monovalent femtomolar antigen-binding affinity. *Proc. Natl Acad. Sci. USA*, **97**, 10701–10705.
 27. Feldhaus, M. J., Siegel, R. W., Opresko, L. K., Coleman, J. R., Feldhaus, J. M., Yeung, Y. A. *et al.* (2003). Flow-cytometric isolation of human antibodies from a nonimmune *Saccharomyces cerevisiae* surface display library. *Nature Biotechnol.* **21**, 163–170.
 28. Kieke, M. C., Cho, B. K., Boder, E. T., Kranz, D. M. & Wittrup, K. D. (1997). Isolation of anti-T cell receptor scFv mutants by yeast surface display. *Protein Eng.* **10**, 1303–1310.
 29. Holler, P. D., Holman, P. O., Shusta, E. V., O'Herrin, S., Wittrup, K. D. & Kranz, D. M. (2000). *In vitro* evolution of a T cell receptor with high affinity for peptide/MHC. *Proc. Natl Acad. Sci. USA*, **97**, 5387–5392.
 30. Kieke, M. C., Shusta, E. V., Boder, E. T., Teyton, L., Wittrup, K. D. & Kranz, D. M. (1999). Selection of functional T cell receptor mutants from a yeast surface-display library. *Proc. Natl Acad. Sci. USA*, **96**, 5651–5656.
 31. Kieke, M. C., Sundberg, E., Shusta, E. V., Mariuzza, R. A., Wittrup, K. D. & Kranz, D. M. (2001). High affinity T cell receptors from yeast display libraries block T cell activation by superantigens. *J. Mol. Biol.* **307**, 1305–1315.
 32. Shusta, E. V., Holler, P. D., Kieke, M. C., Kranz, D. M. & Wittrup, K. D. (2000). Directed evolution of a stable scaffold for T-cell receptor engineering. *Nature Biotechnol.* **18**, 754–759.
 33. Starwalt, S. E., Masteller, E. L., Bluestone, J. A. & Kranz, D. M. (2003). Directed evolution of a single-chain class II MHC product by yeast display. *Protein Eng.* **16**, 147–156.
 34. Schweickhardt, R. L., Jiang, X., Garone, L. M. & Brondyk, W. H. (2003). Structure-expression relationship of tumor necrosis factor receptor mutants that increase expression. *J. Biol. Chem.* **278**, 28961–28967.
 35. Frayser, M., Sato, A. K., Xu, L. & Stern, L. J. (1999). Empty and peptide-loaded class II major histocompatibility complex proteins produced by expression in *Escherichia coli* and folding *in vitro*. *Protein Expr. Purif.* **15**, 105–114.
 36. Boder, E. T. & Wittrup, K. D. (2000). Yeast surface display for directed evolution of protein expression, affinity, and stability. *Methods Enzymol.* **328**, 430–444.
 37. Zhao, H., Shen, Z. M., Kahn, P. C. & Lipke, P. N. (2001). Interaction of alpha-agglutinin and a-agglutinin, *Saccharomyces cerevisiae* sexual cell adhesion molecules. *J. Bacteriol.* **183**, 2874–2880.
 38. LaPan, K. E., Klapper, D. G. & Frelinger, J. A. (1992). Production and characterization of two new mouse monoclonal antibodies reactive with denatured mouse class II beta chains. *Hybridoma*, **11**, 217–223.
 39. Santambrogio, L., Sato, A. K., Fischer, F. R., Dorf, M. E. & Stern, L. J. (1999). Abundant empty class II MHC molecules on the surface of immature dendritic cells. *Proc. Natl Acad. Sci. USA*, **96**, 15050–15055.
 40. Stratmann, T., Apostolopoulos, V., Mallet-Designe, V., Corper, A. L., Scott, C. A., Wilson, I. A. *et al.* (2000). The I-A^{g7} MHC class II molecule linked to murine diabetes is a promiscuous peptide binder. *J. Immunol.* **165**, 3214–3225.
 41. Busch, R. & Rothbard, J. B. (1990). Detection of peptide-MHC class-II complexes on the surface of intact cells. *J. Immunol. Methods*, **134**, 1–22.
 42. Orr, B. A., Carr, L. M., Wittrup, K. D., Roy, E. J. & Kranz, D. M. (2003). Rapid method for measuring ScFv thermal stability by yeast surface display. *Biotechnol. Prog.* **19**, 631–638.
 43. Ueda, M. & Tanaka, A. (2000). Genetic immobilization of proteins on the yeast cell surface. *Biotechnol. Advan.* **18**, 121–140.

44. Hammond, C. & Helenius, A. (1994). Quality control in the secretory pathway: retention of a misfolded viral membrane glycoprotein involves cycling between the ER, intermediate compartment, and Golgi apparatus. *J. Cell Biol.* **126**, 41–52.
45. Chang, J. W., Mechling, D. E., Bachinger, H. P. & Burrows, G. G. (2001). Design, engineering, and production of human recombinant T cell receptor ligands derived from human leukocyte antigen DR2. *J. Biol. Chem.* **276**, 24170–24176.
46. Thomas, A., Meurisse, R. & Brasseur, R. (2002). Aromatic side-chain interactions in proteins. II. Near- and far-sequence Phe-X pairs. *Proteins: Struct. Funct. Genet.* **48**, 635–644.
47. Burley, S. K. & Petsko, G. A. (1986). Amino–aromatic interactions in proteins. *FEBS Letters*, **203**, 139–143.
48. Burley, S. K. & Petsko, G. A. (1988). Weakly polar interactions in proteins. *Advan. Protein Chem.* **39**, 125–189.
49. Zauhar, R. J., Colbert, C. L., Morgan, R. S. & Welsh, W. J. (2000). Evidence for a strong sulfur–aromatic interaction derived from crystallographic data. *Biopolymers*, **53**, 233–248.
50. Reid, K. S. C., Lindley, P. F. & Thornton, J. M. (1985). Sulphur–aromatic interactions in proteins. *FEBS Letters*, **190**, 209–213.
51. Todd, J. A., Bell, J. I. & Mcdevitt, H. O. (1987). HLA-DQ-beta gene contributes to susceptibility and resistance to insulin-dependent diabetes-mellitus. *Nature*, **329**, 599–604.
52. Sato, A. K., Sturniolo, T., Sinigaglia, F. & Stern, L. J. (1999). Substitution of aspartic acid at beta57 with alanine alters MHC class II peptide binding activity but not protein stability: HLA-DQ (alpha1*0201, beta1*0302) and (alpha1*0201, beta1*0303). *Hum. Immunol.* **60**, 1227–1236.
53. Waldburger, C. D., Jonsson, T. & Sauer, R. T. (1996). Barriers to protein folding: formation of buried polar interactions is a slow step in acquisition of structure. *Proc. Natl Acad. Sci. USA*, **93**, 2629–2634.
54. Doebele, R. C., Pashine, A., Liu, W., Zaller, D. M., Belmares, M., Busch, R. & Mellins, E. D. (2003). Point mutations in or near the antigen-binding groove of HLA-DR3 implicate class II-associated invariant chain peptide affinity as a constraint on MHC class II polymorphism. *J. Immunol.* **170**, 4683–4692.
55. Sato, A. K., Zarutskie, J. A., Rushe, M. M., Lomakin, A., Natarajan, S. K., Sadegh-Nasseri, S. *et al.* (2000). Determinants of the peptide induced conformational change in the human class II major histocompatibility complex protein HLA-DR1. *J. Biol. Chem.* **275**, 2165–2173.
56. Natarajan, S. K., Assadi, M. & Sadegh-Nasseri, S. (1999). Stable peptide binding to MHC class II molecule is rapid and is determined by a receptive conformation shaped by prior association with low affinity peptides. *J. Immunol.* **162**, 4030–4036.
57. Ferlin, W., Glaichenhaus, N. & Mougneau, E. (2000). Present difficulties and future promise of MHC multimers in autoimmune exploration. *Curr. Opin. Immunol.* **12**, 670–675.
58. Shusta, E. V., Raines, R. T., Pluckthun, A. & Wittrup, K. D. (1998). Increasing the secretory capacity of *Saccharomyces cerevisiae* for production of single-chain antibody fragments. *Nature Biotechnol.* **16**, 773–777.
59. Zhu, X., Bavari, S., Ulrich, R., Sadegh-Nasseri, S., Ferrone, S., McHugh, L. & Mage, M. (1997). A recombinant single-chain human class II MHC molecule (HLA-DR1) as a covalently linked heterotrimer of alpha chain, beta chain, and antigenic peptide, with immunogenicity *in vitro* and reduced affinity for bacterial superantigens. *Eur. J. Immunol.* **27**, 1933–1941.
60. Horton, R. M., Ho, S. N., Pullen, J. K., Hunt, H. D., Cai, Z. & Pease, L. R. (1993). Gene splicing by overlap extension. *Methods Enzymol.* **217**, 270–279.
61. Oldenburg, K. R., Vo, K. T., Michaelis, S. & Paddon, C. (1997). Recombination-mediated PCR-directed plasmid construction *in vivo* in yeast. *Nucl. Acids Res.* **25**, 451–452.
62. Prado, F. & Aguilera, A. (1994). New *in vivo* cloning methods by homologous recombination in yeast. *Curr. Genet.* **25**, 180–183.
63. Zhao, H., Giver, L., Shao, Z., Affholter, J. A. & Arnold, F. H. (1998). Molecular evolution by staggered extension process (StEP) *in vitro* recombination. *Nature Biotechnol.* **16**, 258–261.
64. Gietz, R. D. & Woods, R. A. (2002). Transformation of yeast by lithium acetate/single-stranded carrier DNA/polyethylene glycol method. *Guide Yeast Genet. Mol. Cell Biol., Part B*, **350**, 87–96.
65. Stern, L. J., Brown, J. H., Jardetzky, T. S., Gorga, J. C., Urban, R. G., Strominger, J. L. & Wiley, D. C. (1994). Crystal structure of the human class II MHC protein HLA-DR1 complexed with an influenza virus peptide. *Nature*, **368**, 215–221.

Edited by I. Wilson

(Received 9 February 2004; received in revised form 16 April 2004; accepted 20 April 2004)